Sequence and Structural Requirements for High-Affinity DNA Binding by the WT1 Gene Product

HITOSHI NAKAGAMA,[1] GUNTHER HEINRICH,[1]† JERRY PELLETIER,[2]
AND DAVID E. HOUSMAN[1]*

*Center for Cancer Research, Massachusetts Institute of Technology, Cambridge,
Massachusetts 02139,[1] and Department of Biochemistry and McGill Cancer
Center, McGill University, Montreal, Quebec, Canada H3G 1Y6[2]*

The Wilms' tumor suppressor gene, *WT1*, encodes a zinc finger polypeptide which plays a key role regulating cell growth and differentiation in the urogenital system. Using the whole-genome PCR approach, we searched murine genomic DNA for high-affinity WT1 binding sites and identified a 10-bp motif 5′GCGTGGGAGT3′ (which we term WTE). The WTE motif is similar to the consensus binding sequence 5′GCG(G/T)GGGCG3′ recognized by EGR-1 and is also suggested to function as a binding site for WT1, setting up a competitive regulatory loop. To evaluate the underlying biochemical basis for such competition, we compared the binding affinities of WT1 and EGR1 for both sequences. WT1 shows a 20- to 30-fold-higher affinity for the WTE sequence compared with that of the EGR-1 binding motif. Mutational analysis of the WTE motif revealed a significant contribution to binding affinity by the adenine nucleotide at the eighth position (5′GCGTGG GAGT3′) as well as by the 3′-most thymine (5′GCGTGGGAGT3′), whereas mutations in either flanking nucleotides or other nucleotides in the core sequence did not significantly affect the specific binding affinity. Mutations within WT1 zinc fingers II to IV abolished the sequence-specific binding of WT1 to WTE, whereas alterations within the first WT1 zinc finger reduced the binding affinity ~10-fold but did not abolish sequence recognition. We have thus identified a WT1 target, which, although similar in sequence to the EGR-1 motif, shows a 20- to 30-fold-higher affinity for WT1. These results suggest that physiological action of WT1 is mediated by binding sites of significantly higher affinity than the 9-bp EGR-1 binding motif. The role of the thymine base in contributing to binding affinity is discussed in the context of recent structural analysis.

The Wilms' tumor (WT) suppressor gene resides at human chromosome 11p13 (16, 37). *WT1* encodes a polypeptide composed of two functional domains: a proline-glutamine-rich amino terminus and four zinc fingers of the Cys₂-His₂ variety at the carboxyl terminus (4). Homozygous disruption of the *WT1* gene in mice (24), as well as some specific germ line WT1 mutations in humans, results in developmental failure of the urogenital system (2, 27, 34, 35). The identification of *WT1* mutations in sporadic and hereditary cases of WT has established the identity of this gene as a tumor suppressor gene (7, 8, 15, 22, 26, 43). These results identify WT1 as a key regulatory molecule essential for differentiation and development of the urogenital system.

The early growth response gene *EGR-1* (also known as *Zif268*) encodes a protein that contains three zinc fingers of the Cys₂-His₂ variety (5) and activates transcription in a sequence-specific manner (28). Zinc fingers II to IV of the WT1 gene product show a high degree of homology (51 to 63%) to the three EGR-1 zinc fingers (4). The structural analysis of EGR-1/Zif 268 has been invaluable in establishing a framework within which to understand the mechanism of DNA binding by WT1. Crystallographic studies of a Zif 268 zinc finger-DNA (5′GCGTGGGCG3′) complex identified three amino acids in each zinc finger that interact with three nucleotides in the major groove of the target DNA sequence (32). This association is mediated through hydrogen bond contacts, most made to the guanine-rich strand. There are a number of key struc-

tural differences, however, within the WT1 DNA binding domain which distinguish it from EGR-1 and suggest that the molecular details of DNA binding are not identical. The first WT1 zinc finger does not have significant homology with any of the three EGR-1 zinc fingers at the amino acid level (4). Additionally, four WT1 isoforms are produced by alternative splice site selection within the coding region of the gene (17). The second alternative splice inserts or removes three amino acids (KTS) between zinc fingers III and IV and changes the DNA binding specificity of the protein (10, 30, 36). Third, amino acid conservation between EGR1 and WT1 is restricted to the zinc fingers with significant differences outside this region possibly affecting the identity and spacing of amino acids with ancillary functions in DNA binding.

Determining the identity of genes controlled by WT1 is essential to understanding its role in controlling differentiation and cell growth. A number of studies have shown that the WT1 isoforms lacking the KTS splice site can bind in vitro to the same target sequence (5′GCGGGGGCG3′) as the EGR-1 protein whereas the KTS isoforms do not (30, 36). To date, several studies have directed their efforts towards the identification of downstream targets of WT1 by scanning known promoter regions for the EGR-1-like consensus sequences (6). With this approach six potential targets have been identified, and they include the genes encoding insulin-like growth factor 2 (IGF-2) (9), platelet-derived growth factor A (PDGF-A) (12), insulin-like growth factor 1 receptor (IGF-1R) (46), colony-stimulating factor 1 (CSF-1) (19), insulin-like growth factor binding protein 2 (IGFBP-2) (20), and WT1 itself (38). Reporter constructs harboring minimal promoters from these genes have shown that they can be negatively or positively regulated by WT1 in transient transfection systems. Addition-

---

* Corresponding author. Phone: (617) 253-3013. Fax: (617) 253-5202.

† Present address: K.O. Technology, Cambridge, MA 02139.

ally, a whole-genome PCR approach (23) has been attempted with the four zinc fingers of WT1 produced in *Escherichia coli* (1). Recently, a (TCC)$_n$ motif has also been identified as a potential binding site for WT1 (44). Although these experiments identified a series of genomic fragments, some of which contained EGR-1-like motifs, a more detailed and precise analysis is required to determine if the EGR-1 consensus site is involved in the biology of WT1.

To address this issue, we have focused on identifying genomic DNA sequences demonstrating a high affinity for WT1. We used in vitro-synthesized full-length WT1 in a whole-genome PCR approach to select high-affinity sites. Herein we describe the nature of one of these sites and characterize the corresponding WT1 and EGR-1 interactions. The characterization of this site has significant implications for the understanding of WT1 function in controlling growth and differentiation.

MATERIALS AND METHODS

Materials and reagents. Restriction endonucleases, the Klenow fragment of DNA polymerase, T4 polynucleotide kinase, and T4 DNA ligase were from New England Biolabs. [5-^{3}H]CTP (25.5 Ci/mmol), [α-^{32}P]dCTP (~3,000 Ci/mmol), and [^{35}S]methionine (1,000 Ci/mmol) were obtained from NEN Research Products. m^{7}GpppG was from Pharmacia, and poly(dI-dC) · poly(dI-dC) were from Boehringer Mannheim. RNase inhibitor (RNasin), RNase-free DNase I, and rabbit reticulocyte lysate were from Promega. *Taq* DNA polymerase was from Cetus. Oligonucleotides were obtained from the Massachusetts Institute of Technology Biopolymer Center.

Construction of WT1 expression vectors. The *Xma*I 1.8-kb fragments of all four isoforms of the murine WT1 cDNA (3) [we refer to them as WT1(−/−), -(−/+), -(+/−), and -(+/+), depending on the presence or absence of the two alternatively spliced sites] were cloned into the *Xma*I site of Bluescript II SK(+) or *Eco*RI-*Xba*I site of pSP65-73A (31). A series of mutants containing alterations in the zinc finger domains of WT1 have been previously described. All mutants, except WAR (18), were made by PCR-based oligonucleotide-mediated mutagenesis, as previously described (21), using the wild-type WT1(−/−) as a template. del-1 is a deletion mutant of all of zinc finger I from Cys-308 to His-330. All mutants have been sequenced with Sequenase (U.S. Biochemical) by the chain termination method (39) to verify the presence of the mutation and the absence of PCR-generated second-site mutations.

In vitro transcription and translation. All cDNA plasmids were purified by CsCl banding. Each plasmid was linearized and transcribed with either T3, T7, or SP6 RNA polymerase, depending on the backbone of the expression vector and orientation of the inserts. Transcription reactions were carried out for 2 h at 37°C as previously described (14). Essentially, reactions were performed in 40 mM Tris-HCl (pH 7.5)–6 mM MgCl$_2$–2 mM spermidine–10 mM dithiothreitol–500 μM each CTP, UTP, and ATP–100 μM GTP, 500 μM m^{7}GpppG–100 μg of bovine serum albumin per ml–3 μl of RNase inhibitor–3 to 5 μg of linearized template DNA in a total reaction volume of 100 μl. As a tracer, ^{3}H-CTP was added to the reaction mix to a final concentration of 4 μM. After the reaction, 5 U of RNase-free DNase I was added, and the samples were incubated for 15 min at 37°C, extracted with phenol-chloroform, purified by passing through a Sephadex G-50 column (fine; Pharmacia), ethanol precipitated, and resuspended in 10 μl of RNase-free water. In vitro-synthesized mRNA (0.5 μg) was translated in rabbit reticulocyte lysate for 1 h at 30°C in the presence or absence of ^{35}S-methionine. The ^{35}S-labelled proteins were electrophoresed in sodium dodecyl sulfate (SDS)-polyacrylamide gels (see Fig. 3A), dried, and exposed either to Kodak X-Omat film or to a PhosphorImager screen. Protein products were quantitated by calculating the intensity of labelled products with a PhosphorImager system (Molecular Dynamics) as well as by trichloroacetic acid precipitation. The in vitro-synthesized protein was aliquoted and stored at −80°C. Protein aliquots were used only once when thawed.

Whole-genome PCR. The selection strategy for identifying a WT1 target sequence is based on the whole-genome PCR approach reported by Kinzler and Vogelstein (23). Briefly, the target DNA fragments were prepared by digesting mouse genomic DNA with *Sau*3A1. The digested DNA was repaired with the Klenow fragment of DNA polymerase and ligated to catch linkers containing *Eco*RI and *Xho*I restriction sites. The linker primers were then used in a PCR to amplify the restricted fragments. All four WT1 isoforms were produced in vitro as described above, and 40 μl of the lysate containing all four WT1 isoforms were mixed with 2 μg of linker-ligated genomic DNA. The binding reaction was carried out in 50 mM HEPES (*N*-2-hydroxyethylpiperazine-*N'*-2-ethanesulfonic acid) (pH 7.5)–50 mM KCl–5 mM MgCl$_2$–10 μM ZnSO$_4$–1 mM dithiothreitol–20% glycerol. The DNA-protein complexes were immunoprecipitated in 50 mM HEPES (pH 7.5)–150 mM KCl–5 mM MgCl$_2$–10 μM ZnSO$_4$–0.5% Triton–0.05% SDS with a rabbit anti-WT1 polyclonal antibody. Following immunopre-

cipitations, the DNA was eluted in 500 mM Tris-HCl (pH 9.0)–20 mM EDTA–10 mM NaCl–0.4% SDS and amplified by the PCR using the catch linkers as primers. We repeated this cycle four times, after which the amplified DNA fragments were introduced into the *Eco*RI site of Bluescript SK(+). Colonies obtained after transfection into DH5α were lifted onto GeneScreen Plus nylon filters (NEN Research Products) and probed with radiolabeled amplified DNA. Probes (50 ng) were prepared by the random primer method (11) in 50 μl at 37°C for 30 min and boiled for 10 min in 200 μl of a solution containing 5× SSC (1× SSC is 0.15 M NaCl plus 0.015 M sodium citrate), and 1 mg of sheared mouse genomic DNA per ml. Repeated sequences were blocked by preannealing for 2 to 4 h at 65°C. Hybridizations were performed for 12 to 24 h at 42°C in 50% formamide–1 M NaCl–10% dextran sulfate–1% SDS–100 μg of salmon sperm DNA per ml–50 ng of labelled probe. The nucleotide sequences of positive clones were determined by the chain termination method using Sequenase.

Mobility shift assays. Probes for mobility shift assays were prepared from clones identified by hybridizations or from synthetic oligonucleotides. Synthetic oligonucleotide probes were prepared by annealing complementary oligonucleotides at 37°C for 30 min. Annealed oligonucleotides were phosphorylated with T4 polynucleotide kinase in the presence of 1 mM ATP and cloned into the *Eco*RV site of Bluescript SK(+), and the nucleotide sequence was determined. Inserts were removed from Bluescript by restricting with *Eco*RI and *Hind*III and purified on an 8% polyacrylamide gel. The amount of recovered fragment was quantitated by measuring the A_{260}. Fragments were end labelled with [α-^{32}P]dCTP by using the Klenow fragment of DNA polymerase. The binding reactions were carried out in a total volume of 15 μl in 50 mM HEPES (pH 7.5)–50 mM KCl–5 mM MgCl$_2$–10 μM ZnSO$_4$–1 mM dithiothreitol–20% glycerol–1 μg of poly(dI-dC) · poly(dI-dC)–0.2 nM (about 10^4 cpm) each DNA probe with various amounts of in vitro-translated WT1 protein ranging from 0 to 4 μl. Following binding, reaction mixtures were electrophoresed on 4% polyacrylamide gels (acrylamide/bisacrylamide ratio, 37:1) in 0.5× TBE (1× TBE is 89 mM Tris–89 mM boric acid–2 mM EDTA) buffer at 150 V for 2 to 3 h at room temperature. For competition experiments, binding reactions were carried out in the presence of a 100-fold molar excess of unlabelled probe added simultaneously with the labelled probe to the reaction mixture. Gels were dried and exposed to Kodak X-Omat film at −70°C or to a PhosphorImager screen. For quantitative binding analysis, the intensity of the mobility shifts were quantitated by Phosphorimaging analysis, and the binding affinity was quantitated as the ratio of bound to unbound probe.

Footprinting analysis. The DNA fragment used for footprinting analysis was prepared from one of the selected clones (clone 76 in Fig. 1) by digesting with *Xho*I and *Pst*I to release the insert. This fragment was then end labelled with [α-^{32}P]dCTP by using the Klenow fragment of DNA polymerase. Approximately 5 × 10^5 cpm (5 ng) of end-labelled probe was mixed with 40 μl of reticulocyte lysate containing in vitro-synthesized WT1(−/−). DNA-protein complexes were resolved as described above and autoradiographed, and both the complexed probe and the free probe were excised from the gel. Gel slices were subjected to cupric sulfate-phenanthroline cleavage as described elsewhere (25). Briefly, the gel slice was submerged in 200 ml of 50 mM Tris-HCl (pH 8.0). Twenty milliliters of 2.0 mM 1,10-phenanthroline monophosphate–0.45 mM CuSO$_4$ and 20 ml of 58 mM mercaptopropionic acid were then added. The digestion was carried out for 10 min at room temperature and quenched by addition of 20 ml of 28 mM 2,9-dimethyl-1,10-phenanthroline. Following chemical cleavage, the DNA was electroblotted onto an NA45 DEAE membrane (Schleicher & Schuell) in 0.25× TBE. The blotted DNA was eluted by incubating at 65°C for 30 min in 20 mM Tris-HCl (pH 8.0)–1 M NaCl–0.1 mM EDTA. The eluted probe was extracted with phenol-chloroform and ethanol precipitated in the presence of 0.3 M NaOAc and 5 mM MgCl$_2$. Similar amounts of bound and unbound probes were loaded onto an 8% sequencing gel and electrophoresed at 1,500 V for ~1 h. Gels were dried and autoradiographed overnight at −70°C. Sequences were aligned by comparison with a G+A Maxam-Gilbert ladder (29) of the probe which was coelectrophoresed in adjacent lanes.

Quantitative analysis of equilibrium DNA binding and Scatchard plot analysis. To estimate the amount of WT1 protein in the reticulocyte lysate participating in the formation of DNA-protein complexes, we performed equilibrium DNA binding analysis using the mobility shift assay. Various amounts of the WT1 programmed lysate (0 to 8 μl) were incubated with 10 pM radiolabelled probe as described above. The total amount of lysate was adjusted to 8 μl by complementing with unprogrammed lysate. Samples were incubated at 4°C for 30 min and analyzed on a 4% polyacrylamide gel.

Scatchard plot analysis (40) was performed to determine the dissociation constant, K_d, from the mobility shift assays. The experiments were performed three times, with similar results. For each experiment, 4 μl of programmed lysate was mixed with increasing concentrations (between 10 pM and 1 nM) of probes. Following resolution by gel electrophoresis, the amounts of radioactivity in the bands corresponding to free and bound DNAs were quantitated by using a PhosphorImager, and the bound/free probe ratio was plotted.

RESULTS

Identification of a WT1 target sequence. Accurate identification of the downstream targets of the WT1 gene product is
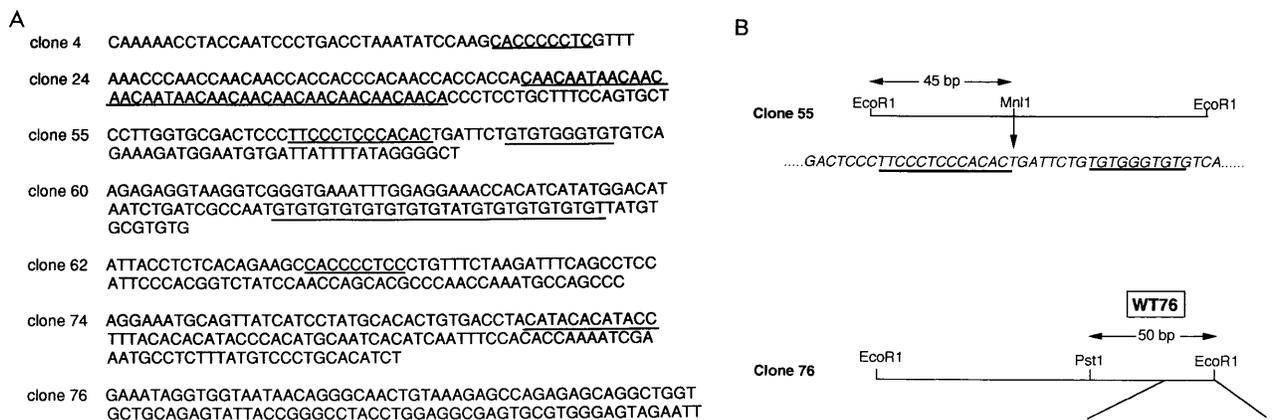
A

clone 4   CAAAAACCTACCAATCCCTGACCTAAATATCCAAG<u>CACCCCCTCG</u>TTT

clone 24 AAACCCAACCAACAACCACCACCCACAACCACCACCA<u>CAACAATAACCAAC</u>
          <u>AACAATAACAACAACAACAACAACAACAACAA</u>CACCCTCCTGCTTTCCAGTGCT

clone 55 CCTTGGTGCGACTCCC<u>TTCCCTCCCACACT</u>GATTCT<u>GTGTGGGTGT</u>GTCA
          GAAAGATGGAATGTGATTATTTTATAGGGGCT

clone 60 AGAGAGGTAAGGTCGGGTGAAATTTGGAGGAAACCACATCATATGGACAT
          AATCTGATCGCCAAT<u>GTGTGTGTGTGTGTGTGTATGTGTGTGTGTGTGTT</u>TATGT
          GCGTGTG

clone 62 ATTACCTCTCACAGAAGC<u>CACCCCTCCC</u>TGTTTCTAAGATTTCAGCCTCC
          ATTCCCACGGTCTATCCAACCAGCACGCCCAACCAAATGCCAGCCC

clone 74 AGGAAATGCAGTTATCATCCTATGCACACTGTGACCTA<u>CATACACATACC</u>
          TTT<u>ACACACATACC</u>CACATGCAATCACATCAATTTCC<u>ACACCAAAATCGA</u>
          AATGCCTCTTTATGTCCCTGCACATCT

clone 76 GAAATAGGTGGTAATAACAGGGCAACTGTAAAGAGCCAGAGAGCAGGCTGGT
          GCTGCAGAGTATTACCGGGCCTACCTGGAGGCGAGT<u>GCGTGGGAGT</u>AGAATT

B

FIG. 1. Whole-genome PCR of DNA fragments showing affinity for WT1. (A) Nucleotide sequences of 7 selected clones out of a total 400 present in the library. Most clones have GC-rich stretches; others have di- or trinucleotide repeats (underlined). (B) Restriction maps of clones 55 and 76. Both clones form specific complexes with WT1 in gel mobility shift assays. Each clone possesses either an *Mnl*I site or a *Pst*I site in the middle of the sequence, which were used to generate shorter fragments to identify the WT1 recognition site.

essential in elucidating the role it plays in normal and abnormal development of the urogenital system. Although the EGR-1 consensus motif has been proposed as a putative binding site for WT1, the affinity of WT1 for this site is much lower (~40-fold) than EGR-1's affinity for the same sequence (34). Consequently, in an attempt to identify physiologically relevant WT1 targets, we have applied the whole-genome PCR approach on murine genomic DNA with all four WT1 isoforms.

The whole-genome PCR approach was performed as described in Materials and Methods. Following amplification by PCR and cloning of selected genomic DNA fragments, 400 clones were obtained, of which ~80 were sequenced. In this report, we present the sequences of seven different fragments characterized in detail (Fig. 1). Clone 24 was the most abundant in the library, and included a (CAA)$_n$ repeat. Clone 60 possesses a (GT)$_n$ repetitive sequence. These repetitive sequences are known to exist redundantly in the genome (42) and may reflect nonspecific binding of WT1 to these elements. Similar nonspecific sequences have been previously identified by using the same approach with WT1 (1). Analysis of these clones was not pursued. Many of the clones identified contain GC-rich stretches showing a significant homology to the EGR-1 core motif, 5′GCG(G/T)GGGCG3′ (Fig. 1A, clones 4, 55, 62, 74, and 76).

Mobility shift assays with selected inserts. To identify the WT1 recognition domain within our clones, a survey of DNA binding to in vitro-synthesized WT1 was performed. Clones 55 and 76 formed specific complexes with WT1 protein. To narrow down the region with which WT1 was interacting, the inserts of clones 55 and 76 were divided into two smaller regions by restriction enzyme digestion (Fig. 1B). The *Eco*RI-*Mnl*I fragment (45 bp) of clone 55, as well as the *Pst*I-*Eco*RI fragment (50 bp) of clone 76 formed specific complexes with WT1 with similar mobilities (data not shown). The subregion of clone 76 gave the most striking result, producing two complexes (I and II) (Fig. 2), both of which were inhibited by a 100-fold molar excess of unlabelled fragment (Fig. 2) but not by mutant EGR-1 oligonucleotides (data not shown). Complex II was thought to arise from a truncated version of WT1 generated by leaky scanning and translation initiation at a downstream in-frame ATG often observed during in vitro translation of WT1. To clarify this point, we constructed a series of 5′

deletions within WT1 and in vitro-translated proteins were used in gel shift assays with the subregion of clone 76 (Fig. 3B and C). The SDS-polyacrylamide gel electrophoresis (SDS-PAGE) analysis of the wild-type WT1 protein (46 kDa) showed the existence of smaller-molecular-weight products, the sizes of which were consistent with those generated by the
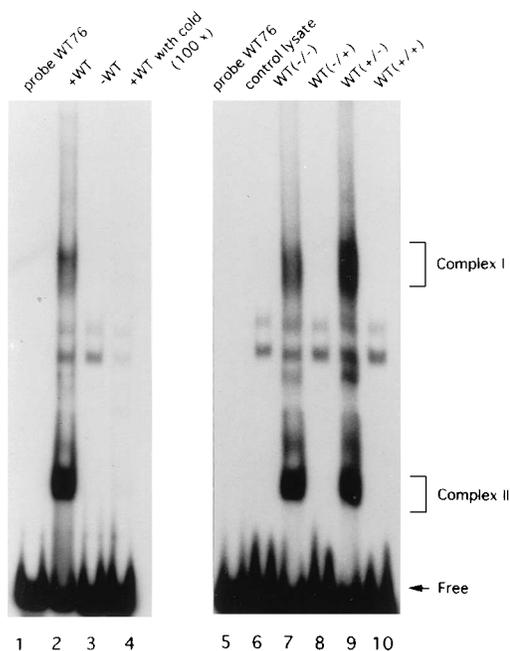

FIG. 2. Complex formation by WT1 with clone 76. Mobility shift assays with the *Eco*RI-*Pst*I fragment (50 bp) of clone 76 and WT1 produced in reticulocyte lysate. Lanes: 1 and 5, no protein; 2 and 7, lysates with WT1(−/−) protein; 3 and 6, unprimed control lysate; 4, lysate with WT1(−/−) and a 100-fold molar excess of unlabelled probe; 8, lysate with WT1(−/+); 9, lysate with WT1(+/−); 10, lysate with WT1(+/+). Two complexes (I and II) are specifically formed. Unbound (free) probe is indicated. Two nonspecific complexes are formed in unprimed reticulocyte lysate. The WT1(−/−) and WT1(+/−) isoforms form specific complexes, whereas the other isoforms do not bind WT76. After electrophoresis the gels were dried and exposed against Kodak X-Omat film at −70°C for 12 to 24 h with an intensifying screen.
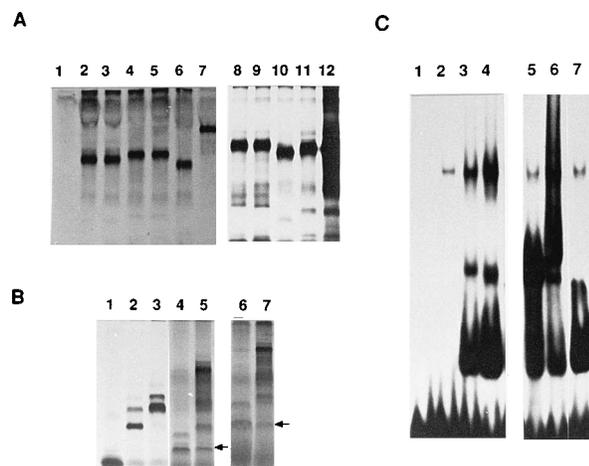
FIG. 3. SDS-PAGE analyses of in vitro-translated WT1 proteins labelled with ^{35}S-methionine. (A) Full-length WT1 proteins including various mutants. Lanes: 1, control; 2, WT($-/-$); 3, WT($-/+$); 4, WT($+/-$); 5, WT($+/+$); 6, WAR, lacking zinc finger 3; 7, EGR-1; 8 to 11, G3, G6, del-1, and WB mutants, respectively (Fig. 9); 12, Drash mutant. (B) In vitro-translated WT1 proteins with 5′-truncated WT1 cDNAs as templates. Lanes: 1, control; 2, WT1 cDNA truncated at the *Nco*I site as a template (TR1); 3, WT1 truncated at the *Bsu*36I site (TR2); 4 and 6, WT1 truncated at the *Rsa*I site (TR3); 5 and 7, full-length WT1. Lanes 1 to 5, 10% polyacrylamide gel; lanes 6 and 7, 15% polyacrylamide gel. Arrows, products of about 18 kDa in lanes 4 and 6, also present in the full-length WT1 translations (lanes 5 and 7). (C) Mobility shift assays of the TR1 to -3 proteins with the WTE oligonucleotide. Lanes: 1, probe only; 2, unprogrammed control lysate; 3, WT($+/-$) lysate; 4, WT($-/-$) lysate; 5, TR1 lysate; 6, TR2 lysate; 7, TR3 lysate.
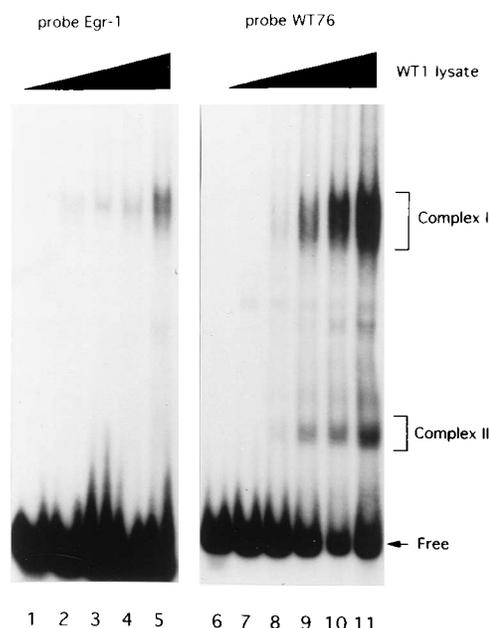

FIG. 4. Comparison of the relative binding affinities of the EGR-1 consensus motif and WT76 for WT1. A 37-bp fragment containing the EGR-1 binding site 5′cccggcGCGGGGGGCGaggcg3′ was excised from Bluescript SK(+) with *Eco*RI-*Hin*dIII and radiolabelled as described in Materials and Methods. The *Pst*I-*Eco*RI 50-bp fragment was excised from clone 76 and radiolabelled with the Klenow fragment of DNA polymerase. Increasing concentrations (triangles) of WT1 protein were added to the binding reaction mixtures. The concentration of the target probe was 0.2 nM, except for lane 11 (0.4 nM). The binding affinity of WT76 was ~30 times higher than that of the EGR-1 binding sequence. After electrophoresis the gel was dried and exposed against Kodak X-Omat film at $-70°$C for 12 to 24 h with an intensifying screen. Lanes: 1 and 6, probe alone; 2 and 7, control lysate; 3 and 8, 1 μl of lysate with WT1($-/-$) protein. Lanes 4 and 9 and lanes 5, 10, and 11, 2 and 4 μl of lysate with WT1($-/-$), respectively. For all reactions, the total amount of lysate was adjusted to 4 μl with unprimed control lysate.

deletion constructs (Fig. 3B). For example, the deletion construct which possesses only the four zinc fingers (Fig. 3B, lane 4) produced a small protein product, also detected when full-length WT1 mRNA was translated (Fig. 3B, arrows). The mobility shift assay with this truncated protein yielded a complex with the same mobility as complex II (Fig. 3C). These data document the occurrence of leaky scanning and translation initiation of WT1 mRNA at the downstream in-frame ATG.

Within clone 76 is a motif similar to the EGR-1 consensus site (Fig. 1B). This sequence, 5′GCGTGGGAG3′, is present near the *Eco*RI site of the cloned insert. On the basis of these initial results, we pursued characterization of clone 76 to better characterize this motif. (Hereafter, we refer to the 50-bp *Pst*I-*Eco*RI fragment of clone 76 as WT76 and to the core GC-rich sequence in WT76, 5′GCGTGGGAGT3′, as WTE).

Characterization of the WT76 binding site. The WT1 gene is alternatively spliced, resulting in the production of four isoforms containing or lacking exon 5 and/or the amino acids KTS in the linker sequence between zinc fingers III and IV (17). To determine if all four WT1 isoforms are capable of forming complexes with WT76, we performed gel shift assays with similar amounts of each isoform. Only the $-$KTS isoforms [WT1($-/-$) and WT1($+/-$)] are capable of interacting with WT76 (Fig. 2B). No differences in binding affinities between WT1($-/-$) and WT1($+/-$) were detected, indicating that the presence of absence of the first alternatively spliced exon (exon 5) does not significantly affect DNA binding. In vitro-synthesized EGR-1 protein was also able to interact with WTE and is characterized in greater detail below (Fig. 4).

To compare the relative affinities of WT1 for WTE and the EGR-1 consensus motif, mobility shift assays were performed in the presence of a constant amount of a radiolabelled target probe and increasing concentrations of protein (Fig. 4). The bound/free probe ratios revealed that WT1 has a ~30-fold-

higher binding affinity for WTE than for the EGR-1 consensus sequence. To demonstrate specificity in binding of WT1 to WTE, a mutational analysis of the WTE sequence was performed. The core motif, 5′GC**G**TGGGAGT3′, was mutated to 5′GC**A**TGGGAGT3′ [WTE(^{3}G→A)] or 5′GCGTG**A**GAGT3′ [WTE(^{6}G→A)]. Previous experiments have shown that converting the EGR-1 motif, 5′GCGGGGGCG3′ to 5′GCGGG**A**GCG3′ abolishes recognition by EGR-1 or WT1 (34). In vitro-synthesized WT1 and EGR-1 are capable of binding to WTE (Fig. 5, lanes 3 and 4), and complex formation is abolished with both mutant WTE sites (Fig. 5, lanes 7, 8, 11, and 12). These results demonstrate that the WTE motif within WT76 is the actual site of WT1 recognition. We sought to directly demonstrate this by using DNA footprinting protection.

Footprinting analysis of WT76. The chemical cleavage footprinting assay using cupric sulfate was performed as detailed in Materials and Methods. Protection by WT1 was detected at the postulated WTE site (5′GCGTGGGAGT3′) (Fig. 6; compare bound- and unbound-probe lanes). Partial protection was observed at the first two upstream nucleotides, 5′**GC**GTGGGAGT3′, as well as at the downstream thymine, 5′GCGTGGGAG**T**3′, since signals with reduced intensities (60 to 70%) were still visible in the bound-probe lane (Fig. 6). Complete protection of the remaining nucleotides within the WTE sequence was observed (Fig. 6; compare unbound- and bound-probe lanes). The protected region thus defined spans 10 nucleotides.
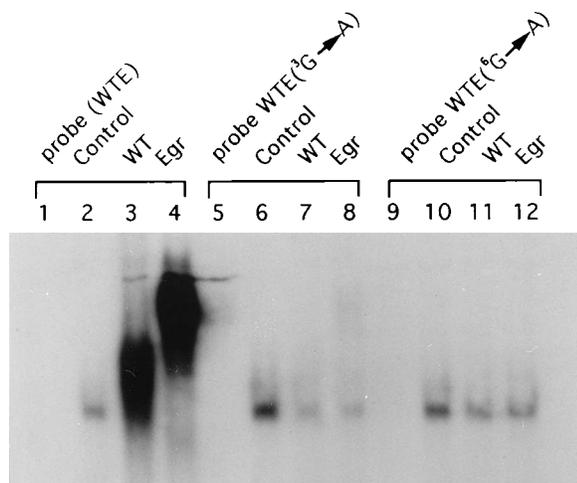
FIG. 5. Structural requirements for complex formation by WTE with WT1. Two WTE mutants, 5′GCATGGGAGT3′ [WTE(³G→A)] and 5′GCGTG AGAGT3′ [WTE(⁶G→A)] were analyzed for complex formation. Rabbit reticulocyte lysates primed with no RNA (lanes 2, 6, and 10), WT1(−/−) mRNA (lanes 3, 7, and 11), or EGR1 mRNA (lanes 4, 8, and 12) were incubated with WTE (lanes 1 to 4), WTE(³G→A) (lanes 5 to 8), or WTE(⁶G→A) (lanes 9 to 12). Lanes 1, 5, and 9, probe alone, with no reticulocyte lysate. After electrophoresis the gel was dried and exposed against Kodak X-Omat film at −70°C for 12 h with an intensifying screen.

Scatchard plot analysis of WT1 binding to WT76. To quantitate the binding affinities, we performed equilibrium DNA binding to achieve saturation of the WTE site by WT1 protein synthesized in vitro. Each experiment was performed at least three times, yielding reproducible binding affinities. Figure 7A demonstrates the mobility retardation assay with increasing concentrations of WT1 protein. The intensity of the complexes (I and II) increased proportionally with the amount of WT1 protein added to the reaction mixtures. A bound/free probe ratio of 0.5 was achieved with ∼2 μl of the lysate for complex I. The binding reaction was also carried out with excess probe, ranging from 10 pM to 1 nM, to evaluate the dissociation constant. The dissociation constant (K_d, calculated by Scatchard plot analysis) of the WT1 binding sequence was approximately 0.5 nM (Fig. 7B and C). The lower complex (complex II) had a similar binding affinity (data not shown). We failed to derive a K_d value for the interaction of WT1 with the EGR-1 consensus motif, because of the low affinity WT1 has for this site. We estimate this binding affinity to be at least 20-fold lower than the affinity of WT1 for the WTE site.

Contextual effects on the binding affinities of WTE for WT1. To define at the nucleotide level which bases were contributing to WT1-DNA complex formation, we generated a series of oligonucleotides containing point mutations within, or adjacent to, the WTE sequence (5′cgagtGCGTGGGAGTagaa tt3′). Each probe was 21 nucleotides in length, containing 10 bases of the core WTE sequence flanked by the same nucleotides present in WT76. A variety of point mutants in which WTE, or two residues downstream of the WTE sequence, were targeted were generated. We also synthesized the EGR-1 binding site (5′cccggcGCGGGGGCGagggcg3′) previously used to assess WT1-DNA interactions (28, 36).

Since footprinting experiments revealed partial protection of a thymine residue in the WTE site (Fig. 6), it is possible that this nucleotide plays a role in stabilizing protein-DNA complex formation. Thus, to determine if this residue was an actual contact site or if its protection was fortuitous, probes differing
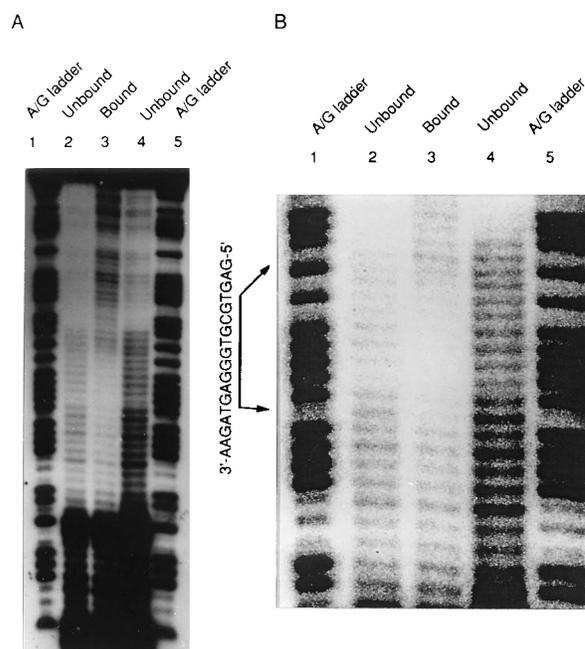

FIG. 6. (A) Footprint protection of the *Xho*I-*Pst*I fragment (152 bp) of clone 76 by WT1. The DNA probe was end labelled with [α-³²P]dCTP by using the Klenow fragment of DNA polymerase. For each experiment, 5×10^5 cpm (∼5 ng) of probe was used for the mobility shift-based footprinting. Lanes 1 and 5, Maxam-Gilbert sequence ladder (A/G cleavage) of the target fragment (3,000 cpm); lanes 2 and 4, footprinting patterns with unbound probes (3,000 and 9,000 cpm of the input fragment, respectively); lane 3, footprinting pattern with isolated complex I (3,000 cpm). Protection was detected within the 5′GCGTGG GAGT3′ core, and a PhosphorImager printout of the protected area is shown at a higher magnification in panel B. An 8% sequencing gel was used to resolve the nucleotide fragments and, following drying, was exposed to Kodak X-Omat film at −70°C for 48 h.

at this residue were prepared and incubated with WT1 protein. Specific complex formation was decreased slightly (∼3-fold) when thymine (5′GCGTGGGAG**T**3′) was converted to a cytosine residue (5′GCGTGGGAG**C**3′) but severely affected (>10-fold) when thymine was converted to an adenine residue (5′GCGTGGGAGA**A**3′) (Fig. 8A, upper panel), which is present at the same position in the EGR-1 binding sequence. Although the similar T nucleotide preference was observed with EGR-1 protein, the effect on the binding affinity was 2- to 3-fold for EGR-1 in contrast to 20-fold for WT1. WT1 protein showed a drastic deterioration in binding affinity after a substitution at T-10 (Fig. 8B). Mutations converting the downstream nucleotide adjacent to the thymine from an adenine (5′GCGTGGGAGT**A**G3′) to a thymine (5′GCGTGGGAGT **T**G3′) or a guanine (5′GCGTGGGAGT**G**G3′) only slightly affected the binding affinities (approximately twofold) (Fig. 8A, upper panel).

We also tested oligonucleotide probes containing nucleotide substitutions at various sites in the EGR-1-like core sequence. Of the various probes tested, WT1 protein showed the highest affinity to WTE (5′GCGTGGGAGT3′) (Fig. 8A, lower panel). Changing the second cytosine to adenine (5′G**A**GTGGGA GT3′) in WTE had no effect on binding. Mutating the eighth adenine to cytosine (5′GCGTGGG**C**GT3′) or guanine (5′GC GTGGG**G**GT3′) within this core had a mild effect on affinity, decreasing the bound/free probe ratio approximately twofold. Mutating the fourth thymine in the WTE sequence to a cytosine (5′GCG**C**GGGAGT3′) significantly decreased the
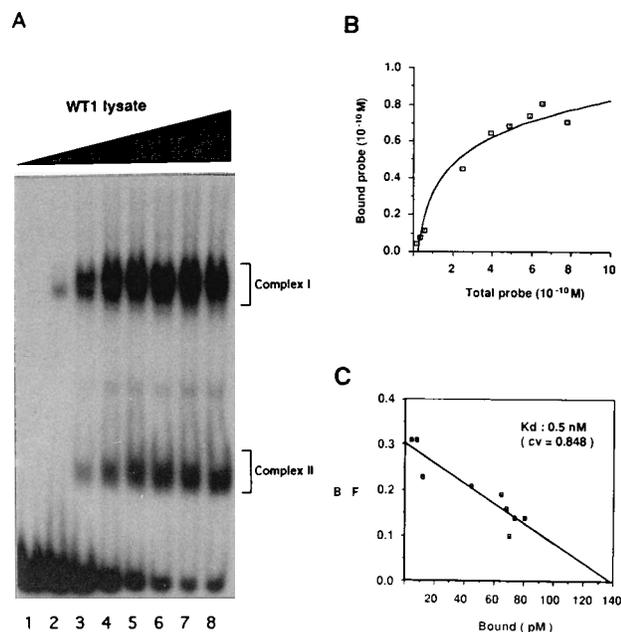
FIG. 7. (A) Saturation binding analysis of WT1 with the WT76 DNA probe. Increasing amounts of reticulocyte lysate programmed with WT1(−/−), ranging from 0 to 8 μl, were used with 10 pM of radiolabelled WT76. The increasing amounts of WT1(−/−) protein are indicated (triangle). Lanes: 1, probe only; 2, control lysate; 3 to 8, 1, 2, 3, 4, 6, and 8 μl of lysate with WT1(−/−), respectively. To calculate binding affinity, the bound/free probe (B/F) ratio was calculated as described in Materials and Methods. Under these conditions, 50% complex formation was obtained with 2 μl of the WT1(−/−) lysate (lane 4). Saturation was reached with 6 μl of WT1 lysate. (B and C) Saturation binding study varying the amount of WT76 probe from 10 pM to 1 nM with Scatchard plot analysis. Results for a representative experiment are shown in panel C. Three experiments were performed, all of which gave similar results (K_d, 0.4 to 1.0 nM). cv, coefficient of variation.

binding affinity. The EGR-1 consensus sequence failed to show even minimal binding to WT1 (>20-fold decrease in affinity) (Fig. 8A, lower panel). We also compared the core nucleotide preference for the binding between WT1 and EGR-1 protein using the oligonucleotides containing the WTE flanking sequences (Fig. 8B). EGR-1 showed the highest affinity for the EGR-1 core sequence, and WT1 showed the highest affinity for the WTE sequence. Interestingly, the A-8→G substitution decreased EGR-1 binding approximately eightfold (compare lane 6 with lane 7 in Fig. 8B), whereas WT1 showed only a 30 to 40% decrease in binding affinity with this nucleotide substitution (compare lane 5 with lane 7). As shown in Fig. 8B, the WTE sequence possessed the highest affinity for WT1 protein and the G-8 substitution showed more specific binding to WT1 than to EGR-1, although not of the highest affinity.

Mutations in nucleotide sequence upstream of the WTE site did not significantly affect protein-DNA complex formation (data not shown). These results suggest that the nature of the last thymine nucleotide within the WTE motif has a significant influence on high-affinity binding to WT1, with the core sequence contributing specificity between WT1 and EGR-1.

The first WT1 zinc finger contributes significantly to DNA recognition. To date, experiments aimed at elucidating WT1 structural features responsible for DNA binding have focused mainly on zinc fingers II to IV, notably because of their homology to the EGR-1 zinc fingers (4). Zinc finger I shows little homology to the EGR-1 fingers, and its role in DNA recognition, if any, is not well understood. To define WT1 structural motifs required for efficient DNA recognition, a variety of

mutations within this domain were constructed (Fig. 9A). Mutations consisted of (i) alterations of key histidine residues within the four zinc fingers (mutants G1 to G6), (ii) deletions of zinc fingers (mutants del-1 and WAR), and (iii) missense mutations previously defined in Denys-Drash syndrome and postulated to abolish DNA binding (mutants WB and Drash). Mobility shift experiments with in vitro-synthesized proteins from the various mutants revealed that specific protein-DNA complexes were detected only with G5, WB, and del-1. Mutations affecting the integrity of zinc fingers II to IV completely abolished DNA binding (Fig. 9B). Mutant G5 has two histidine residues converted to cysteines and changes the spacing between zinc fingers I and II. Mutant WB has a G-to-A transition within zinc finger I, converting a cysteine residue to a tyrosine. Mutant del-1 lacks zinc finger I. Although a small amount of complex I was observed with these three mutants, it is clear that the binding affinities of these mutant WT1 proteins are greatly reduced (~90%) compared with intact WT1 (Fig. 9B; compare lane 5 with lane 3 and lanes 12 and 13 with lane 11). Small amounts of a new complex were detectable with mutant del-1 (Fig. 9B, lane 12), likely due to the removal of 23 amino acids from the internally initiated truncated WT1 product. This complex is more apparent in Fig. 10 (lanes 8 and 9).

To evaluate the contribution of the 10th-nucleotide thymine in the interaction with the WT1 finger I and to demonstrate the specificity of complex formation, WB and del-1 proteins were incubated with oligonucleotides containing an adenine or cytosine permutation at the 10th position of the WTE sequence. These substitutions decrease the affinity of wild-type WT1 for WTE but do not abolish it (Fig. 10; compare lane 3 with lanes 1 and 2). Both finger I mutant proteins inefficiently formed complexes with the mutated oligonucleotides, compared with the wild-type WTE sequence (Fig. 10; compare lane 6 with lanes 4 and 5 and lane 9 with lanes 7 and 8). These results demonstrate that complex formation with finger I mutants WB and del-1 has the same nucleotide requirements as wild-type WT1 as well as directly demonstrate a significant contribution of WT1 zinc finger I to DNA recognition and binding.

DISCUSSION

Previous attempts at defining WT1 target sequences have documented that WT1 can bind to EGR-1 and EGR-1-like sequences (28, 36). Database searches for promoter elements containing EGR-1 motifs, followed by transient transfection assays, have identified IGF-2, PDGF-A, IGF-1R, IGFBP-2, CSF-1, and WT1 itself as possible target genes of WT1 (9, 12, 19, 20, 38, 46). Consequently, models expanding the view that WT1 and EGR-1 cross-regulate each other's target genes in cells in which both proteins are expressed have been proposed. To date, however, no direct in vivo experimental evidence suggesting that these genes are bona fide targets of WT1 exists. We have used whole-genome PCR to identify a genomic fragment with a higher affinity for WT1 than that of the classical EGR-1 motif. Footprinting analysis revealed protection within a 10-nucleotide sequence, 5′GCGTGGGAGT3′, which we refer to as WTE. Quantitative mobility shift assay and Scatchard plot determination of the dissociation constant revealed an affinity at least 20-fold higher than that for the EGR-1 motif.

Whole-genome PCR has been previously used to search for WT1 binding sites (1). With this method, two genomic fragments with EGR-1-like motifs have been identified. Although capable of forming complexes with the +KTS and −KTS WT1 isoforms, these fragments failed to demonstrate specific competition with excess unlabelled oligonucleotides. Additionally, DNA fragments with (GT)$_n$ repeats were identified. More re-
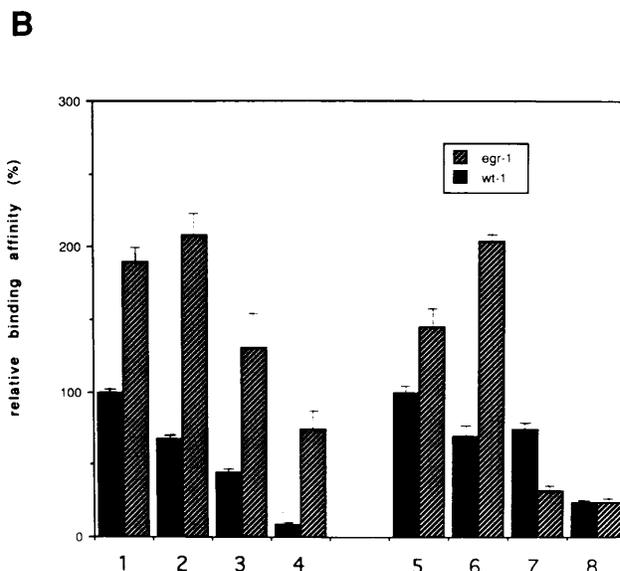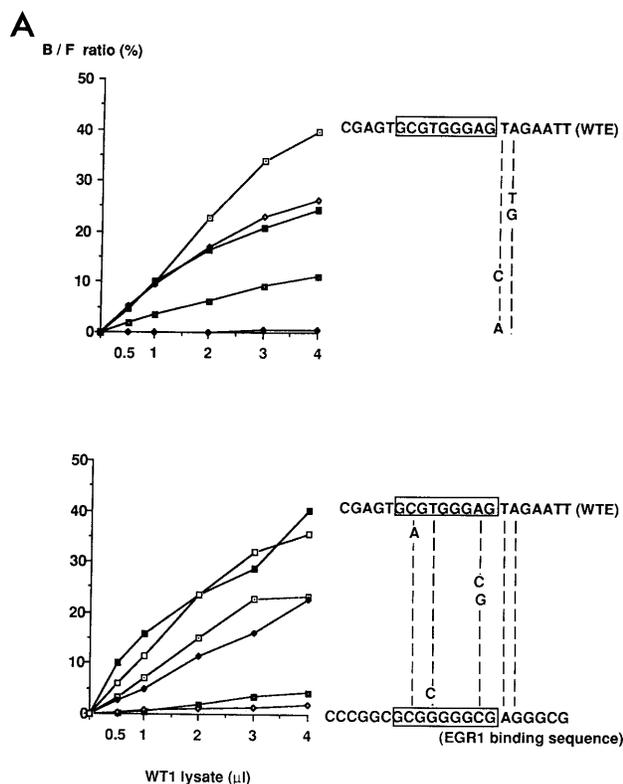
FIG. 8. Binding affinities of different motifs for WT1($-/-$). (A) Mobility shift assays were performed with WT1-programmed reticulocyte lysate and various oligonucleotide sequences containing substitutions downstream of the EGR-1-like motif in the core WTE sequence (upper panel). Binding reactions were carried out with increasing amounts of WT1 lysate (0, 0.5, 1, 2, 3, and 4 μl) and 0.2 nM each probe. Mobility shift assays were also performed with oligonucleotides containing substitutions in the EGR-1-like motif of the core WTE sequence (5′GCGTGGGAG3′) (lower panel). B/F, bound probe/free probe. (B) Relative binding affinities of WT1 and EGR-1 for oligonucleotides containing substitutions of the flanking sequence (bars 1 to 4) or the core sequence (bars 5 to 8). Bars 1 and 5, gel shifts with the WTE sequence (cgagtGCGTGGGAGTagaatt); bar 2, EGR-1 core sequence with WTE flanking sequences (cgagtGCGGGGGCGTagaatt); bar 3, EGR-1 sequence with an A-10→T substitution (cccggcGCGGGGGCGTgggcg); bar 4, EGR-1 sequence (cccggcGCGGGGGCGAggcg); bar 6, WTE core with an A-8→C substitution (cgagtGCGTGGGCGTagaatt); bar 7, WTE with an A-8→G substitution (cgagtGCGTGGGGGGTagaatt); bar 8, WTE with a T-4→C substitution (cgagtGCGCGGGAGTagaatt). Each experiment was done in triplicate at the same time. The binding affinity for each oligonucleotide was calculated as a percentage of the affinity of the WTE sequence.

cently, (TCC)$_n$ tracts have also been proposed as putative binding sites for WT1 (44). The physiological relevance of these sites to WT1 biology remains to be determined. That WT1 binds to EGR-1 motifs was inferred from the ability to select EGR-1-like motifs from a pool of degenerate oligonucleotides with bacterially produced WT1 zinc fingers. Sequences identified in this fashion contained several permutations at the nucleotide level relative to the core EGR-1 motif (36). All of these elements are capable of forming complexes in the presence of large amounts (200 ng) of recombinant protein. Unfortunately, most of these binding studies have been done with bacterially produced WT1 zinc fingers instead of in vitro-synthesized full-length WT1, and binding affinities were not evaluated to determine the relative strengths of these sequences. Since the identified motifs showed strong sequence similarity to the EGR-1 site, the experimental focus became centered on this core sequence.

According to the crystallographic model of Zif 268–DNA interaction, each zinc finger contacts three nucleotides within the target DNA sequence via three amino acid residues (see Fig. 11). The amino acid alignments in WT1 zinc fingers II to IV are quite similar to the three EGR-1 zinc fingers. By applying the Zif 268–DNA complex model (32) to WT1, we were able to identify similar features with respect to WT1-DNA interactions. The first triplet in the binding core sequence (5′GCG3′) is considered to be recognized by the most C-terminal finger, IV, and the following triplets, 5′TGG3′ and 5′GAG3′, are recognized by fingers III and II, respectively. Our experiments indicate that zinc finger II of WT1 prefers 5′GAG3′ over 5′GCG3′ and 5′GGG3′, since substitution of this site in the WTE sequence to yield 5′GCGTGGG(C/G)GT3′ reduced the affinity twofold. WT1 zinc finger II has an amino acid alignment of RSDQLKR at the essential position

for the DNA contact site, compared with RSDELTR for EGR-1. In EGR-1, the two arginine (R) residues are involved with hydrogen bonding to the two guanine residues in the subsite, 5′**GCG**3′. Our data suggest that there may be additional specificity conferred by amino acids within WT1 zinc finger II, to give preference to 5′GAG3′ versus 5′G(C/G)G3′ binding. Moreover, 5′GAG3′-to-5′GGG3′ substitution gave a lower binding affinity with EGR-1 than with WT1, which showed only a twofold decrease in binding affinity. This added specificity may be due to the presence of a glutamine residue in WT1, but not in EGR-1, at amino acid 352 (RSD**Q**LKR). Such an adenine (A)-glutamine (Q) interaction has previously been proposed in the interaction of the *Drosophila* chorion transcription factors I and II (13, 41).

Our data also demonstrate a clear role for the first zinc finger of WT1 in sequence recognition. Deletion of this finger, or site-directed mutagenesis affecting residues predicted to chelate zinc, decreases the efficiency of DNA-protein complex formation (~10-fold). The importance of this finger to WT1 biology is underscored by the identification of a germ line missense mutation affecting a cysteine residue (and presumably Zn^{2+} binding) associated with Denys-Drash syndrome, a developmental disorder resulting in abnormal urogenital system development and predisposition to WTs (2, 34). If WT1 zinc finger I is also involved directly in DNA recognition, then one would predict that the contiguous triplet next to the WTE site should be protected by footprinting analysis, yielding a
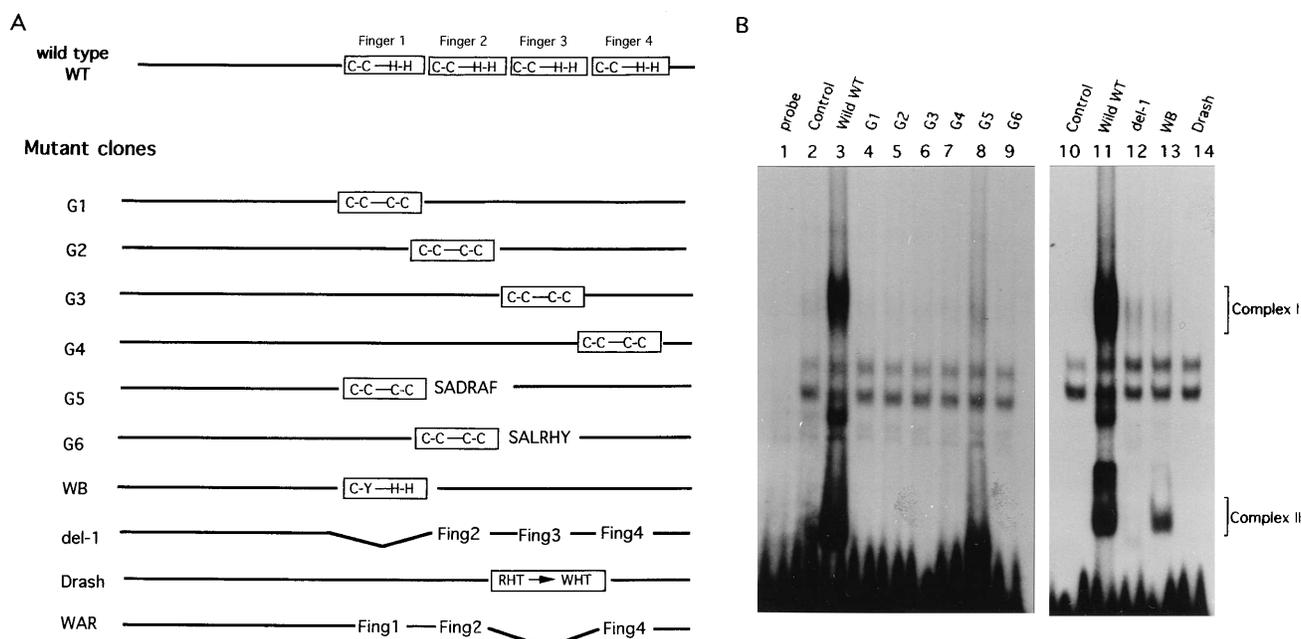
FIG. 9. DNA binding studies with WT1 zinc finger mutants. (A) Schematic diagram of the mutant WT1 constructs. Mutants G1 to G4 have two changes (both His residues are converted to Cys) in each zinc finger. G5 and G6 have the same mutations as G1 and G2, respectively, and also mutations in the spacer sequence either between zinc fingers I and II (TGEKPY→SADRAF) (G5) or between fingers II and III (TGVKPF→SALRHY) (G6). WB contains a point mutation in zinc finger I previously identified in a patient with Denys-Drash syndrome (2), del-1 is a deletion mutant of zinc finger I, Drash has a previously described missense mutation in zinc finger III (37), and WAR is a mouse-human chimeric cDNA (17) lacking zinc finger III, previously identified in a WT (14). All mutations are on the WT1(−/−) backbone. (B) Mobility shift assays of WT1 mutants with a radiolabelled WTE probe. Lane 1, probe alone; lanes 3 to 9 and 11 to 14, WTE probe and reticulocyte lysate programmed with the indicated WT1 mutants. Two nonspecific complexes are present, as judged by their presence in unprimed control lysate (lanes 2 and 10). Following electrophoresis, the gel was dried and exposed against Kodak X-Omat film at −70°C for 24 h with an intensifying screen.

12-bp, rather than 10-bp, protected fragment, as also recently suggested by Drummond et al. (10). Surprisingly, only one additional nucleotide, a thymine, was found to be partially protected in the footprinting assay. Our results indicate that the identity of this nucleotide (T) is important in imparting specificity, since altering its identity decreased binding affinity (Fig. 8A, upper panel). The lack of a clear footprint at this nucleotide may indicate that the interaction between zinc finger I and the 3′-most T in WTE may not be tight enough to be recognized in such an analysis. Alternatively, this finger may not directly interact with DNA. Experiments assaying DNA binding in WT1 mutants with alterations within finger I (WB and del-1) demonstrating the same base pair requirement as with the wild-type WT protein (Fig. 10) are not consistent with a direct role of finger I in DNA binding. Another possibility stems from a recent model of GLI-DNA complexes by Pavletich and Pabo (33). In this model, they described the involvement of a hydrogen bond contact in the zinc finger-DNA complex made by Asp residues at position 2 in the zinc finger helices. According to this model, the Asp (D) residues in Zif 268 fingers interact with adenine or cytosine residues on the opposite strand. If we apply this model to the WT1-WTE interaction, WT1 zinc fingers II to IV contain, at position 2 of the alpha-helix, Asp residues which may interact with adenine or cytosine residues (A-10, C-7, and A-4, respectively) on the opposite strand of WTE, 5′GCGTGGGAGT3′ (Fig. 11). Currently, we do not understand the physical properties of WT1 zinc finger I, which mediates sequence specificity. Like the first finger of the GLI-DNA complex, WT1 finger I may play a key role in stabilizing nucleotide recognition by finger II through protein-protein interactions or structural stabilization of the entire DNA binding domain (33). Of the genes identified as
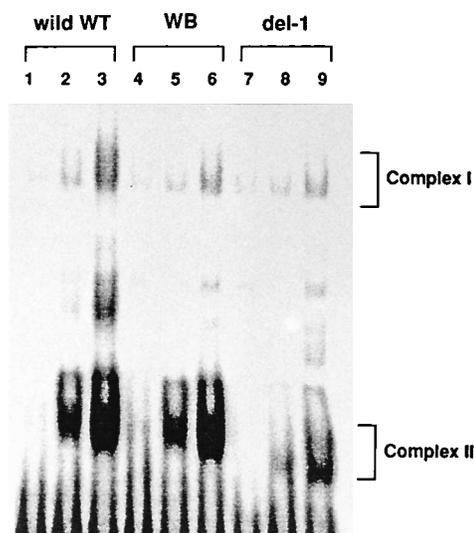

FIG. 10. Specificity of complex formation with WT1 mutants WB and del-1. Complex formation was performed as described in Materials and Methods. The WTE (lanes 3, 6, and 9), WTE T-10→C mutant (5′GCGTGGGAGC3′) (lanes 2, 5, and 8), and WTE T-10→A mutant (5′GCGTGGGAGA3′) (lanes 1, 4, and 7) binding sites were analyzed for their ability to form complexes with reticulocyte lysate programmed with either WT1(−/−) (lanes 1 to 3), WB (lanes 4 to 6), or del-1 (lanes 7 to 9). The positions of complex I and complex II are indicated. After electrophoresis, the gel was dried and exposed against Kodak X-Omat film at −70°C for 24 h with an intensifying screen.
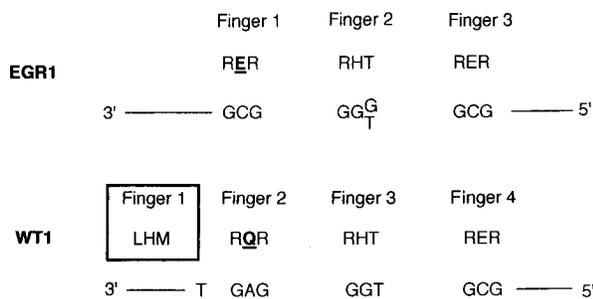
FIG. 11. The predicted DNA-amino acid interactions of WT1 and its cognate sequence based on the crystallographic model of a Zif 268–DNA complex. The amino acids predicted to directly interact with DNA have been aligned with their cognate nucleotides within the core recognition domain and underlined. Possible subsites which interact with individual fingers are shown. The spacing between WT1 zinc fingers I and II is the same as those between fingers II to IV.

putative downstream targets of WT1, PDGF-A and IGFBP-2 have the favorable T flanking the 9-bp EGR-1 motif and PDGF-A, CSF-1, IGFBP-2, and WT1 possess a 5′GAG3′ or 5′GGG3′ instead of 5′GCG3′ at the 3′ end of the binding site in their promoter sequences.

Drummond et al. also elucidated the clear role of the first zinc finger in DNA recognition by analyzing the IGF-2 P3 promoter region (10). In that study they identified the recognition sequence (5′GGC3′) for finger I, which confers the highest binding affinity for WT1 as part of the 12-bp recognition site in the P3 promoter region. They also suggested a clear contribution of finger I to an entirely new binding specificity for a mutant WT1 which possesses only fingers I, II, and IV as a result of an in-frame deletion of finger III. However, the binding affinities measured by equilibrium dissociation constants (K_d) were relatively low compared with that in our study, and moreover, the finger I deletion did not show a significant effect on DNA recognition by fingers II to IV. The discrepancy in relation to our results may be explained by the difference in the amounts of protein and the protein species used for each assay. We used in vitro-translated full-length WT1 protein instead of using bacterially produced zinc fingers of WT1.

Our experiments are aimed at a better understanding of DNA binding of WT1. The importance of this functional property is underscored by the fact that most WT1 mutations in sporadic WTs or Denys-Drash syndrome occur within this domain (2, 7, 15, 26, 34, 35). Whether the WTE site is used in vivo by WT1 is currently under investigation, but it is clear that sequences which demonstrate a substantially higher affinity for WT1 than the canonical EGR-1 motif exist. Our results question the physiological significance of analyzing EGR-1 core motifs in promoter elements as a means of identifying downstream genes under the regulation of WT1, since these sites may have binding affinities quite low relative to other motifs not yet identified. The ability to achieve *trans* repression in transient transfection assays is not quantitative and will not discriminate between low- and high-affinity sites, particularly in the presence of excess effector protein. Clearly, more general and less biased screening methods need to be adopted. These experiments are aimed at identifying the target promoters specific for WT1, rather than EGR1, in order to clarify some of the biology associated with WT1 expression and misexpression.

ACKNOWLEDGMENTS

REFERENCES

1. **Bickmore, W. A., K. Oghene, A. H. Little, A. Seawright, V. van Heyningen, and N. D. Hastie.** 1992. Modulation of DNA binding specificity by alternative splicing of the Wilms tumor wt1 gene transcript. Science **257:**235–257.
2. **Brueing, W., B. Bardeesy, B. L. Silverman, R. A. Cohn, G. A. Machin, A. J. Aronson, D. Housman, and J. Pelletier.** 1992. Germline intronic and exonic mutations in the Wilms' tumour gene (WT1) affecting urogenital development. Nat. Genet. **1:**144–148.
3. **Buckler, A., J. Pelletier, D. A. Haber, T. Glaser, and D. E. Housman.** 1991. Isolation, characterization and expression of the murine Wilms' tumor gene (WT1) during kidney development. Mol. Cell. Biol. **11:**1707–1712.
4. **Call, K. M., T. Glase, C. Y. Ito, A. J. Buchler, J. Pelletier, D. A. Haber, I. A. Rose, A. Kral, H. Yeger, W. H. Lewis, C. Jones, and D. E. Housman.** 1990. Isolation and characterization of a zinc finger polypeptide gene at the human chromosome 11 Wilms' tumor locus. Cell **60:**509–520.
5. **Christy, B., L. F. Lau, and D. Nathans.** 1988. A gene activated in mouse 3T3 cells by serum growth factors encodes a protein with zinc finger sequences. Proc. Natl. Acad. Sci. USA **85:**7857–7861.
6. **Christy, B., and D. Nathans.** 1989. DNA binding site of the growth factor-inducible protein Zif268. Proc. Natl. Acad. Sci. USA **86:**8737–8741.
7. **Coppes, M. J., G. J. Liefers, P. Paul, H. Yeger, and B. R. G. Williams.** 1993. Homozygous somatic WT1 point mutations in sporadic unilateral Wilms tumor. Proc. Natl. Acad. Sci. USA **90:**1416–1419.
8. **Cowell, J. K., R. B. Wadey, D. A. Haver, K. M. Call, D. E. Housman, and J. Prichard.** 1991. Structural rearrangements of the WT1 gene in Wilms' tumor cells. Oncogene **6:**595–599.
9. **Drummond, I. A., S. L. Madden, P. Rohwer-Nutter, G. I. Bell, V. P. Sukhatme, and F. J. Rauscher III.** 1992. Repressin of the insulin-like growth factor II gene by the Wilms tumor suppressor WT1. Science **258:**674–678.
10. **Drummond, I. A., H. D. Rupprecht, P. Rohwer-Nutter, J. M. Lopez-Guisa, S. L. Madden, F. J. Rauscher III, and V. P. Sukhatme.** 1994. DNA recognition by splicing variants of the Wilms' tumor suppressor, WT1. Mol. Cell. Biol. **14:**3800–3809.
11. **Feinberg, A. P., and B. Vogelstein.** 1983. A technique for radiolabeling DNA restriction fragments to high specific activity. Biochem. Biophys. Res. Commun. **111:**47–54.
12. **Gashler, A. L., D. T. Bonthron, S. L. Madden, F. J. Rauscher III, T. Collins, and V. P. Sukhatme.** 1992. Human platelet-derived growth factor A chain is transcriptionally repressed by the Wilms tumor suppressor WT1. Proc. Natl. Acad. Sci. USA **89:**10984–10988.
13. **Gogos, J. A., T. Hsu, J. Bolto, and F. C. Kafotos.** 1992. Sequence discrimination by alternatively spliced isoforms of a DNA binding zinc finger domain. Science **257:**1951–1955.
14. **Green, M. R., T. Maniatis, and D. A. Melton.** 1983. Human b-globin pre-mRNA synthesized in vitro is accurately spliced in Xenopus oocyte nuclei. Cell **32:**681–684.
15. **Haber, D. A., A. J. Buckler, T. Glaser, K. M. Call, F. Pelletier, R. L. Sohn, E. C. Douglass, and D. E. Housman.** 1990. An internal deletion within an 11p13 zinc finger gene contributes to the development of Wilms' tumor. Cell **61:**1257–1269.
16. **Haber, D. A., and D. E. Housman.** 1992. The genetics of Wilms' tumor. Adv. Cancer Res. **59:**41–68.
17. **Haber, D. A., R. L. Sohn, A. J. Buckler, J. Pelletier, K. M. Call, and D. E. Housman.** 1991. Alternative splicing and genomic structure of the Wilms tumor gene WT1. Proc. Natl. Acad. Sci. USA **88:**9618–9622.
18. **Haber, D. A., H. T. M. Timmers, J. Pelletier, P. A. Sharp, and D. E. Housman.** 1992. A dominant mutation in the Wilms tumor gene WT1 cooperates with the viral oncogene E1A in transformation of primary kidney cells. Proc. Natl. Acad. Sci. USA **89:**6010–6014.
19. **Harrington, M. A., B. Konicek, A. Song, X.-L. Xia, W. J. Fredericks, and F. J. Rauscher III.** 1993. Inhibition of colony-stimulating factor-1 promoter activity by the product of the Wilms' tumor locus. J. Biol. Chem. **268:**21271–21275.
20. **Heinrich, G., H. Nakagama, A. L. Brown, M. M. Rechler, and D. E. Housman.** Submitted for publication.
21. **Higuchi, R.** 1990. Recombinant PCR, p. 177–183. *In* M. A. Innis, D. H. Gefland, J. J. Sninsky, and T. J. White (ed.), PCR protocols: a guide to methods and applications. Academic Press, New York.
22. **Huff, V., H. Miwa, D. A. Haber, K. M. Call, D. E. Housman, L. C. Strong, and G. F. Saunders.** 1991. Evidence for WT1 as a Wilms' tumor (WT1) gene: intragenic germinal deletion in bilateral WT. Am. J. Hum. Genet. **48:**997–1003.
23. **Kinzler, K. W., and B. Vogelstein.** 1989. Whole genome PCR: application to the identification of sequences by gene regulatory proteins. Nucleic Acids Res. **17:**3645–3653.
24. **Kreidberg, J. A., H. Sariola, J. M. Loring, M. Maeda, J. Pelletier, D. Housman, and R. Jaenisch.** 1993. WT-1 is required for early kidney devel-

opment. Cell **74:**679–691.

25. **Kuwabara, M. D., and D. S. Sigman.** 1987. Footprinting DNA-protein complexes in situ following gel retardation assays using 1,10-phenanthroline-copper ion: Escherichia coli RNA polymerase-lac promoter complexes. Biochemistry **26:**7234–7238.

26. **Little, M. H., J. Prosser, A. Condie, P. J. Smith, V. V. Heyningen, and N. D. Hastie.** 1992. Zinc finger point mutations within the WT1 gene in Wilms tumor patients. Proc. Natl. Acad. Sci. USA **89:**4791–4795.

27. **Little, M. H., K. A. Williamson, M. Mannens, A. Kelsey, C. Gosden, N. D. Hastie, and V. van Heyningen.** 1993. Evidence that WT1 mutations in Denys-Drash syndrome patients may act in a dominant-negative fashion. Hum. Mol. Genet. **2:**259–264.

28. **Madden, S. L., D. M. Cook, J. F. Morris, A. Gashler, V. P. Sukhatme, and F. J. Rauscher III.** 1991. Transcriptional repressin mediated by the WT1 Wilms tumor gene product. Science **253:**1550–1553.

29. **Maxam, A. M., and W. Gilbert.** 1977. A new method for sequencing DNA. Proc. Natl. Acad. Sci. USA **74:**560–564.

30. **Morris, J. F., S. L. Madden, O. E. Tournay, D. M. Cook, V. P. Sukhatme, and F. J. Rauscher III.** 1991. Characterization of the zinc finger protein encoded by the WT1 Wilms' tumor locus. Oncogene **6:**2339–2348.

31. **Munroe, D., and A. Jacobson.** 1990. mRNA poly(A) tail, a 3′ enhancer of translational initiation. Mol. Cell. Biol. **10:**3441–3455.

32. **Pavletich, N. P., and C. O. Pabo.** 1991. Zinc finger-DNA recognition: crystal structure of a Zif268-DNA complex at 2.1A. Science **252:**809–817.

33. **Pavletich, N. P., and C. O. Pabo.** 1993. Crystal structure of a five-finger GLI-DNA complex: new perspectives on zinc fingers. Science **261:**1701–1707.

34. **Pelletier, J., W. Bruening, C. E. Kashtan, S. M. Mauer, J. C. Manivel, J. E. Striegel, D. C. Houghton, C. Junien, R. Habib, L. Fouser, R. N. Fine, B. L. Silverman, D. A. Haber, and D. E. Housman.** 1991. Germline mutations in the Wilms' tumor suppressor gene are associated with abnormal urogenital development in Denys-Drash syndrome. Cell **67:**437–447.

35. **Pelletier, J., W. Bruening, F. P. Li, D. A. Haber, O. Glaser, and D. E. Housman.** 1991. WT1 mutations contribute to abnormal genital system development and hereditary Wilms' tumour. Nature (London) **353:**431–434.

36. **Rauscher, F. J., J. F. Morris, O. E. Tournay, D. M. Cook, and T. Curran.** 1990. Binding of the Wilms tumor locus zinc finger protein to the EGR-1 consensus sequence. Science **250:**1259–1262.

37. **Rose, E. A., T. Glaser, C. Jones, C. L. Smith, W. H. Lewis, K. M. Call, M. Minden, E. Champagne, L. Bonetta, H. Yeger, and D. E. Housman.** 1990. Complete physical map of the WAGR region of 11p13 localizes a candidate Wilms' tumor gene. Cell **60:**495–508.

38. **Rupprecht, H. D., I. A. Drummond, S. L. Madden, F. J. Rauscher III, and V. P. Sukhatme.** 1994. The Wilms' tumor suppressor gene WT1 is negatively autoregulated. J. Biol. Chem. **269:**6198–6206.

39. **Sanger, F., S. Nicklen, and A. R. Coulson.** 1977. DNA sequencing with chain-terminating inhibitors. Proc. Natl. Acad. Sci. USA **74:**5463–5467.

40. **Scatchard, G.** 1949. The attraction of proteins for small molecules and ions. Ann. N. Y. Acad. Sci. **51:**660–672.

41. **Seeman, N. C., J. M. Rosenberg, and A. Rich.** 1976. Sequence-specific recognition of double helical nucleic acids by proteins. Proc. Natl. Acad. Sci. USA **73:**804–808.

42. **Stallings, R. L., A. F. Ford, D. Nelson, D. C. Torney, C. E. Hildebrand, and R. K. Moyziz.** 1991. Evolution and distribution of (GT)n repetitive sequences in mammalian genomes. Genomics **10:**807–815.

43. **Tadokoro, K., H. Fuji, A. Ohshima, Y. Kakizawa, K. Shimizu, A. Sakai, K. Sumiyoshi, T. Inoue, Y. Hayashi, and M. Yamada.** 1992. Intragenic homozygous deletion of the WT1 gene in Wilms' tumor. Oncogene **7:**1215–1221.

44. **Wang, Z.-Y., Q.-Q. Qiu, K. T. Enger, and T. F. Deuel.** 1993. A second transcriptionally active DNA-binding site for the Wilms tumor gene product, WT1. Proc. Natl. Acad. Sci. USA **90:**8896–8900.

45. **Wang, Z.-Y., Q.-Q. Qiu, and T. F. Deuel.** 1993. The Wilms' tumor gene product WT1 activates or suppresses transcription through separate functional domains. J. Biol. Chem. **268:**9172–9175.

46. **Werner, H., G. G. Re, I. A. Drummond, C. P. Sukhatme, F. J. Rauscher III, D. A. Sens, A. J. Barvin, D. LeRoith, and C. T. Roberts, Jr.** 1993. Increased expression of the insulin-like growth factor I receptor gene, IGFIR, in Wilms tumor is correlated with modulation of IGFIR promoter activity by the WT1 Wilms tumor gene product. Proc. Natl. Acad. Sci. USA **90:**5828–5832.